Experimental study of the thermal performance of a PCM in heat sinks

L. Betancur-Arboleda[1], P. Hulse[2], K. G. Domiciano[2], L. Krambeck[2], M. Mantelli[2]

[1] Faculty of Natural Sciences of Engineering, Unidades Tecnológicas de Santander, Student Street 8-92, Bucaramanga, 680005, Colombia

[2] Heat Pipe Laboratory, Department of Mechanical Engineering, Federal University of Santa Catarina, Florianópolis, SC, 88040-460, Brazil

ABSTRACT

Phase change materials (PCMs) can be great solutions as heat sink for energy storage in microgravity conditions. To guarantee the reliability of the systems, the thermal behavior of the PCMs and their degradation should be understood. Two different configurations of heat sink devices, a cylindrical and a finned hollow parallelepiped based on phase change material (PCM), were investigated. The hydrated salt sodium phosphate dibasic dodecahydrate ($Na_2HPO_4 \cdot 12H_2O$) was used as the PCM material, in three different volumes. Were also investigated the effect of copper sponges in the effective thermal conductivity, and the thermal property degradation in the finned heat sink by the sequential heat cycles. The PCM was replaced in each experiment and two power supply heat flux levels were studied. In the second heat sink configuration, consisting of finned heat sink hollow block provided with internal fins, the PCM was not replaced, to observe its property degradation. Power supplied in finned devices varied from 75W to 100W. Experimental results showed a reduction of approximately 50% in the maximum temperature of the heat sink when the copper sponge is inserted. Gaps in hydrated salt decrease the thermal conductance of the heat sink. The PCM thermo-physical properties degradation is negligible for a few numbers of continuous heating cycles. In the case of finned block device, it was observed a variation of 6% in latent heat storage at the first cycles when the same test was realized several times. Contact area loss increased up 15% at the end of the experiments.

| **Keywords**: | Phase change material, energy storage, hydrated salt. |

Corresponding Author:

Luis Alonso Betancur Arboleda
Faculty of Natural Sciences of Engineering
Unidades Tecnológicas de Santander
Student Street 8-92, Bucaramanga, 680005, Colombia
E-mail: labetancur@correo.uts.edu.co

1. Introduction

Experiments, designed for tests under microgravity conditions, present several limitations due to weight, size and number of components allowed on board of the testing vehicles, such as sounding rockets [1]. Besides, the replacement of materials or damaged parts, during previous to launching qualification tests, is limited, which means that the performance of all experiment components must be well known a priori. Commonly, experiments involving heat transfer devices in microgravity conditions require a heat sink for energy storage, such as phase change materials (PCM), a latent heat storage method. Besides the high energy storage capacity, mainly advantage of PCMs consists in the constant temperature of the phase change [2], it can stabilize the heat sink temperatures [3], but its application is limited due to the thermophysical property degradation and its phase segregation [4], [5]. In addition, density differences between solid and liquid state yields a decreasing in

the contacting area between PCM and the heat exchanger device. Hydrated salts are promising inorganic PCMs, especially in temperature applications below 100°C, due its prominent advantages of large thermal energy storage capacity, low price, rich and easy to obtain, non-toxic and non-flammability, besides its cleaner production [6]. However, these materials present technological challenges to solve, before consider it reliable, both under gravity and under microgravity conditions. According to references [7] and [8], some of these disadvantages of salt-hydrates that require attention are the corrosion of metal, supercooling and the phase separation. Reference [9] affirms that the low thermal conductivity and thermal instability of the salt hydrates, can result in unsatisfactory performance, especially for extended thermal cycling. Both the supercooling and the phase separation can cause a storage capacity degradation if the PCM is not able to solidify or melt between the process temperature range of charging and discharging [7]. A well designed PCM heat sink must be able to keep its temperature as close as possible to the melting temperature of the selected hydrated salt and should avoid the decrease of the contact area between PCM and the heat exchanger, during the fusion process of the dry salt, improving the heat exchange between PCM and the tested device.

Energy storage have been widely studied nowadays especially due its high applicability also in renewable energy systems. Reference [10], for example, studied the effect of radial fins in an annulus cylinder type for latent thermal energy storage, and concluded that the thermal performance improves considerably. Reference [11] demonstrated that the use of copper foam and other solid matrixes increased the thermal conductivity of the PCM thermal control device. Reference [12] investigated the behavior of PCM thermal storages, using three types of solid meshes (triangle, square and hexagonal). The perimeter or area of these solid matrix were maintained the same as well as the amount of phase change material. They concluded that the time taken for the complete melting of PCM is the shortest for the triangular mesh, followed by the rectangular and, finally, hexagonal. Reference [8] studied a new copper foam/hydrated salt composite PCM as supporting matrix for thermal energy storage, and based in the discussions about the thermal conductivity and thermal stability of the composite, they concluded, among other things, that copper foam/SAT composite PCM is promising due its good thermal stability, low supercooling degree and high thermal conductivity. Reference [13] studied the improvement of thermal and heat transfer characteristics through the mixture of different inorganic salt hydrates. Reference [14] combined sodium acetate trihydrate (SAT) with xanthan gum and copper foam to prepare a composite PCM in order to improve its thermal conductivity. Reference [15] analyzed the thermal performance of a mobilized thermal energy storage system applied to renewable energy or to recover the industrial waste heat. The system consisted of sodium acetate trihydrate as phase change material (PCM) filled into a tube-in-tank heat exchanger. Thermal efficiency estimated by the author was about 79,4%. Reference [16] evaluated computationally the effect of different numbers and distributions of fins of consecutive melting and solidification of a PCM in a horizontal double tube. Reference [17], developed a new type of hot water collector tank with a new finned-type cell structure and compared the performance of PCM-loaded finned cell-based tank with PCM-loaded no finned tank and the standard insulated tank. The authors concluded that the finned tank presented an improvement of 10% in relation to the standard tank and of 4-5% to the no-finned tank. Reference [7] charged and discharged the storage of a prototype at different mass flow rates over a fixed temperature range duration. The authors analyzed the presence of phase separation and supercooling and observed a gradual decrease of the effective storage capacity associated with it.

In the present paper, to improve the knowledge of PCM thermal performance and its degradation, two heat sink devices are experimentally studied in the laboratory. The heat sinks have different geometries, one cylindrical and another finned, and they utilize the hydrated salt sodium phosphate dibasic dodecahydrate ($Na_2HPO_4 \cdot 12H_2O$) as the PCM material.

2. Material and methods

Provide sufficient detail to allow the work to be reproduced. Methods already published should be indicated by a reference: only relevant modifications should be described.

2.1. A. Phase change materials (PCM)

The phase change material (PCM) analyzed in this experimental work is the hydrated salt sodium phosphate dibasic dodecahydrate ($Na_2HPO_4 \cdot 12H_2O$). The hydrated salt consists of pellets with heterogeneous crystal particle sizes, which is the original form supplied by the manufacturer, without any compression or melting. Table 1 shows the thermophysical properties of the PCM. For the sample preparation, the PCM material was inserted in two conditions: solid (pellets) and liquid (melted).

Table 1. Sodium phosphate dibasic dodecahydrate properties

Thermo-physical properties	Literature (Farid et al., 2004)	Experimental
Specific heat C_p [kJ/kg°C]	2	
Latent heat γ_{sl} [kJ/kg]	254	
Apparent density of solid ρ_s [kg/m^3]	--	851 ± 10
Liquid density ρ_l [kg/m^3]	--	1664 ± 10
Thermal conductivity k [W/m.°C]	0.5	
Melting temperature T_m [°C]	36	

2.2. Experimental apparatus

Two different experimental heat sinks are used in this research: the first one consists of a cylindrical recipient with an electrical resistor located coaxially, and the second one consists of a fin-based device, with two resistances located at its bottom. Power in both cases is supplied by TDK lambda GEN300-17 equipment. Data acquisition is performed through NI SCXI-1000 equipment and the interface is controlled by Lab-view® 2013.

2.2.1. Cylindrical heat sink

This apparatus consists of a brass cylindrical recipient filled with the PCM and a heater in the center. The recipient dimensions are 71 mm of external diameter (OD), 0.3 mm of wall thickness, and 70 mm of length. The heater consists of an electrical resistance of 567 Ω, 9.52 mm of external diameter, and 67 mm in length. The resistance cartridge is located coaxially, as shown
Figure 1. The container includes a copper sponge matrix in some tests, looking to improve the effective thermal conductivity of the device. The copper sponge has undefined external geometry, varying between 0.5 x 1.0 and 1.0 x 1.0 mm of cross-section. Due to the variated configurations, different quantities of sodium phosphate dibasic dodecahydrate are used to fill. The external surface of the cylinder is isolated with mineral wool. Temperature is measured by 5 Type T thermocouples (± 1°C of uncertainty) equally spaced, embedding into the salt and sealing with silicon to avoid damages. In
Figure 1, T1 is located over the cartridge heater external surface. T2, T3, and T4 are installed in uniform distances in the radial direction over a small radial rod, provided to accommodate the thermocouples. T5 is installed at the internal surface of the recipient. The differences in the device configuration are presented in Table 2.
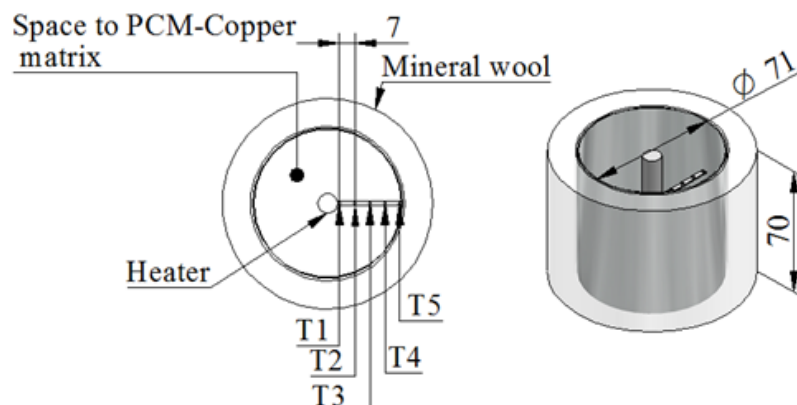
Figure 1. Cylindrical setup [mm]

Table 2. Cylindrical heat sink parameters and test procedures

PCM component	Mass [g]	Salt condition	Filling type	Copper sponge matrix [g]	Power [W]	Heat flux [W/cm^2]	Time [s]
Case 1	183.6 ± 1.0	New	Solid PCM	0	3.4 ± 0.1	15.9	3600
Case 2	396.0 ± 1.0	New	Melted PCM	0	3.4 ± 0.1	15.9	3600
Case 3	360.2 ± 1.0	New	Melted PCM	77.9 ± 1.0	3.4 ± 0.1	15.9	3600
Case 4	360.2 ± 1.0	Used in case 3	Melted case 3	77.9 ± 1.0	7.0 ± 0.1	31.8	12600

2.2.2. Finned heat sink

The fin-based heat sink setup involves a hollow parallelepiped aluminum block of 130 x 700 x100 mm, assisted by 9 (nine) fins, much larger than the cylindrical heat sink. One lateral wall is made of an acrylic sheet, which allows the visualization of the interior region of the block, as shown in Figure 2. Two parallel electrical resistances embedded in rectangular copper blocks supply the heat at the bottom. The resistances have an external diameter of 10 mm, a length of 100 mm length, and equivalent electrical resistance of 76.4 ± 1.0 Ω. The copper block dimensions are 120 x 20 x 20 mm. The free spaces between fins are filled with 714.0 ± 1.0 g of phosphate dibasic dodecahydrate in the liquid state. As in the cylindrical setup, the temperatures are measured by 9 (nine) sealed thermocouples embedded into the salt, preventing deterioration due to contact with hydrated salt. Thermocouples 1 to 6 are located in the middle fin, as shown in Figure 2. The cartridge heater temperature is measured with T7 and T8. The last thermocouple measures the ambient temperature. The finned heat sink parameters are shown in Table 3.
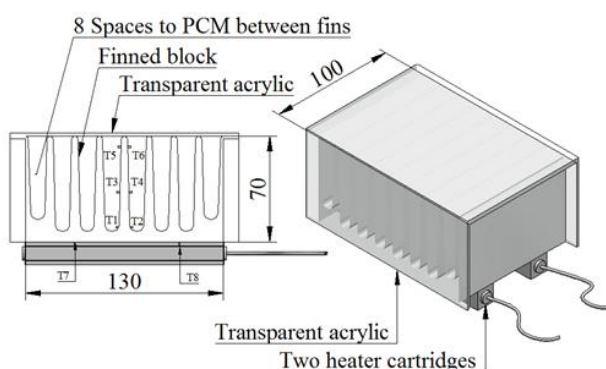
Figure 2. Experimental setup of the fin-based sink [mm]

Table 3. Finned heat sink configurations and test procedures

PCM component	Mass [g]	Number of tests	Salt	Power [W]	Heat flux [W/cm^2]	Time [s]
Case 5	0	1	--	100 ± 2	1.25	1000
Case 6	714.0 ± 1.0	1	New	100 ± 2	1.25	1000
Case 7	714.0 ± 1.0	10	Used in case 6	75 ± 2	1.7	3600

2.3. Experimental procedure

The experiment procedures vary for each studied case. The dissipated power and the duration of each test are presented in Table 2 and Table 3, for cylindrical and finned heat sink, respectively. One should note that the power levels were selected considering a maximum heat flux to be dissipated by the PCM heat sink, considering the future application in microgravity experiments. For the tests depicted in Table 2, after each test, the recipient was emptied, cleaned, and refilled with a new hydrated salt for the next test. The exception

was Case 4 that used the same hydrated salt as Case 3. In fin-based heat sink tests, the degradation of the thermal properties is evaluated, so the hydrated salt is not replaced. The tests were performed with ten heat cycles of one hour and cooling periods of at least 48 hours. The power supply in the finned device varied from 75 W to 100 W, considering long-term tests and flight simulation tests, respectively.

3. Results and discussion

3.1. Cylindrical heat sink results

Case 1: This test configuration involves the deposition of the PCM salt pellets in the empty cylindrical heat sink space. There is a great amount of air between the pellets that acts as a thermal insulator. Figure 3 shows the temperature profiles during the test. The cartridge temperature increases rapidly and ripping when compared to the other temperatures. The reason for that is the gaps and poor contact between the PCM material and the cartridge surface. One should note that the relative difference of densities between the PCM in pellets and liquid states is very high (almost 50%, according to Table 1). So, when the solid PCM melts, its volume decreases, creating voids. The gaps reduce the ability to act as a heat sink, as both the air and salt have low thermal conductivities (see Table 1). In this case, the salt did not melt completely, as thermocouples 3, 4, and 5 show temperatures lower than the salt melting temperature.
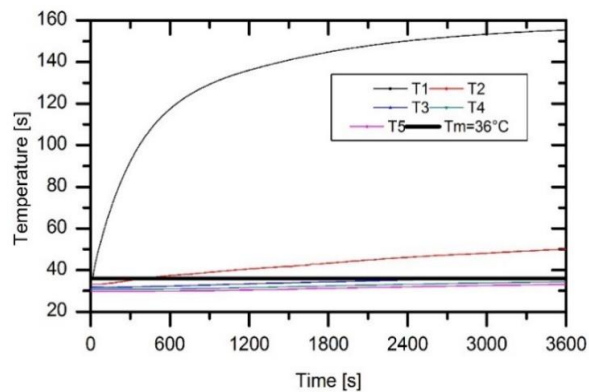
Figure 3. Case 1: Temperature profile of the cylindrical heat sink with PCM in pellets without copper sponge

Case 2: In the second experimental test, the pellets were melted before inserted into the recipient. The thermal equilibrium between the PCM and the ambient air was achieved (20°C) to initiate the test procedure.

Figure 4 presents the thermal behavior of the PCM. After 2000 seconds, the temperature T1 is lower than the same one for Case 1. The better salt accommodation into the container provides a higher salt-heater contact, increasing the heat dissipation. In addition, comparing the thermocouple T1 of Case 1 and Case 2, the maximum temperature decreased from approximately 80°C to 60°C. Besides that, the temperature of thermocouple T2 shows an increasing trend, above 36°C (PCM melting temperature, see Table 1), indicating that the melted PCM in this region. The thermocouples 3, 4, and 5 show a slow increase in the temperatures when compared to Case 1. However, without achieving the melting temperature.
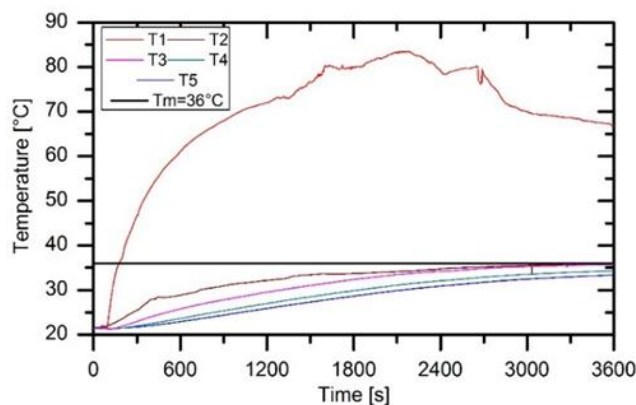
Figure 4. Case 2: Temperature profile with melted PCM without copper sponge

Case 3: The third case consist of the cylindrical heat sink with a copper sponge to improve the thermal conductivity. As in the case 2, the PCM was melted before add-ed. Figure 5 illustrates the thermal performance results from case 3. All temperatures increases while 3.4 W is applied. At 3600 seconds, the temperature (T1) achieves a maximum of 60°C, 10°C lower than the maximum temperature measured in Case 2. No salt accommodation and temperature decreasing were observed.
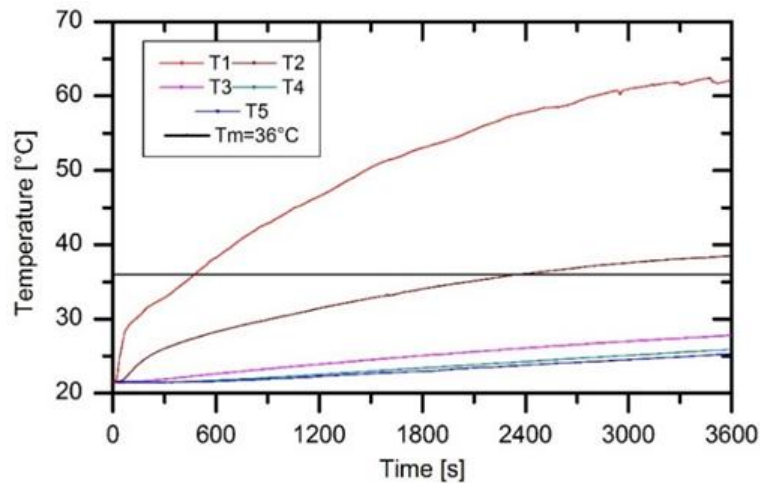
Figure 5. Case 3: Temperature profile with melted pellets of PCM with copper mesh

Case 4: Figure 6, with the same configuration from case 3 but subjected to six power input (7 W) heating cycles for 3.5 hours, shows the temperature profile device. The objective of the test was to verify the performance of the PCM before degrading. Thermocouples T3, T4, and T5 measured almost uniform temperatures proximately to the salt melting temperature (~ 36°C). The maximum temperature (T1) at the heater surface remained almost the same for all the cycles. Temperature oscillations occurred when small particles of salt felt close to the thermocouple.
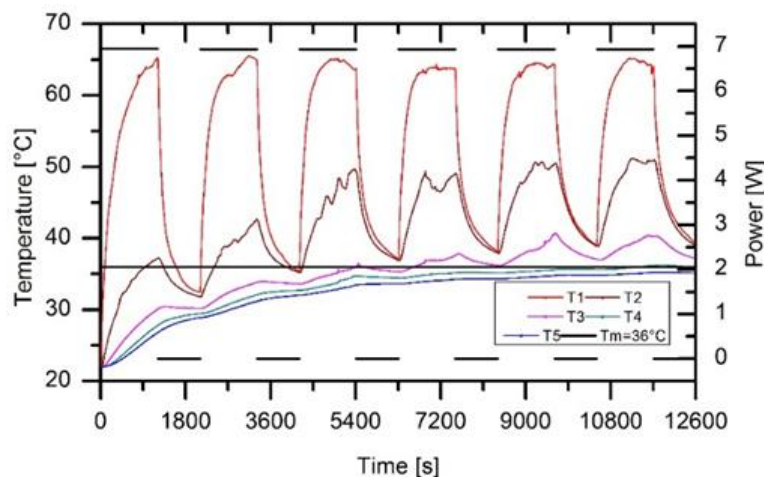
Figure 6. Case 4: Temperature profile with melted pellets of PCM with copper sponge

3.2. Fin-based Heat Sink

Case 5 and Case 6: Figure 7 illustrates the temperature measurement for the empty device subjected to natural air convection. The results show a rapid increase in the temperature distribution, reaching the maximum value allowed, 85 °C, at 1000 seconds.

Figure 8 shows the temperature distribution of the device with PCM. Although the system does not reach the steady-state condition, the highest cylindrical cartridge surface temperature was around 45°C, a reduction of almost 45%, when compared to the previous case (Figure 7).
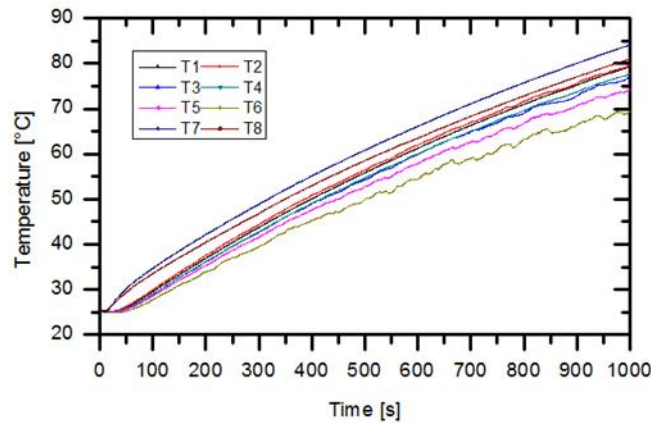
Figure 7. Temperature profile of fin-based device at natural convection
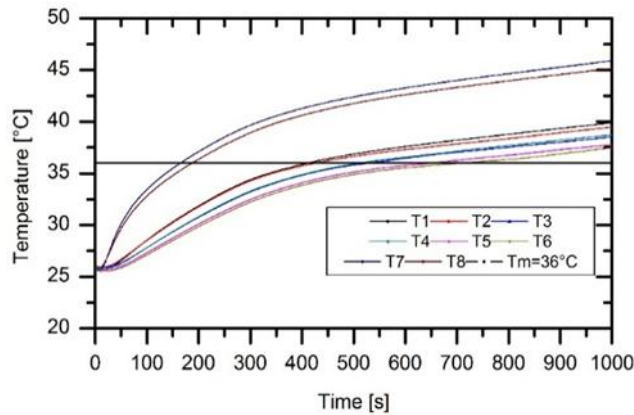
Figure 8. Temperature profile of fin-based and filled with PCM material

Case 7: The degradation of the PCM thermal-physical properties was analyzed, testing it ten times with an identical procedure. Between each test, it waited long enough for the salt to solidify again. The contact losses between salt and walls were minimized by filling the hydrated salt at its liquid state and waited for solidification. The liquid salt shrinks during the solidification process by almost 5% of the total volume, caused by the different densities between liquid and solid phases.

Figure 9 shows several photos of the PCM melting process taken at an interval of 600 seconds. In the beginning,

Figure 9 demonstrates free space between the heat sinks after the PCM solidification. The melting process starts at 2400 seconds. Images from 2400 to 3600s show a defined interface liquid-solid. At 3000 and 3600s, the image shows the complete melting of the salt.
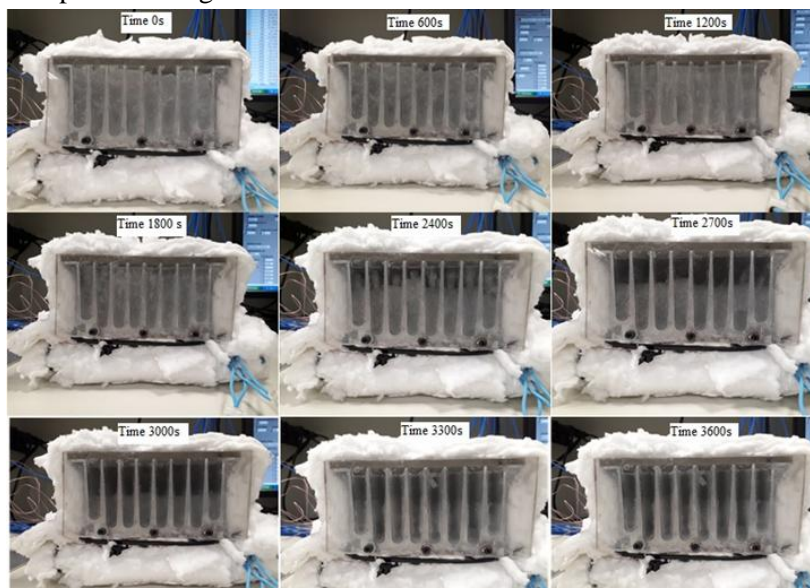
Figure 9. Phase change in case finned heat sink device

Figure 10 shows the results of the proposed tests. In all figures, the elapsed time observed to start the phase change from solid to liquid was similar, around 600 seconds. The phase change phenomena finished at 2400 seconds in the first test, but in tests 2, 3, and 4, this phenomenon ended at 2100 seconds, decreasing the latent heat storage capacity of approximately 6%. Tests from 5 to 8 and 9 to 10 the phase change phenomena period decreased to 1800 and 1200 seconds. The resulted latent heat storage capacity was reduced by approximately 50%.

Besides the melting profile difference, the final temperature observed in the tests increased almost 5°C from each experimental procedure to another. In all testes, the liquid-solid interfaces have similar behavior to those observed in
Figure 9. The free space shown in
Figure 9 slightly increases between the solidification cycles, but this variation is neglected. The liquid volume in the fourth test decreased by almost 17% of the total volume. This volume was estimated using a geometric method, measuring the void space observed over the acrylic sheet. The tenth solidification resulted in a void volume of approximately 17%, representing a loss of the contacting surface between the salt and heat sink of ~15%, as shown in Figure 11.
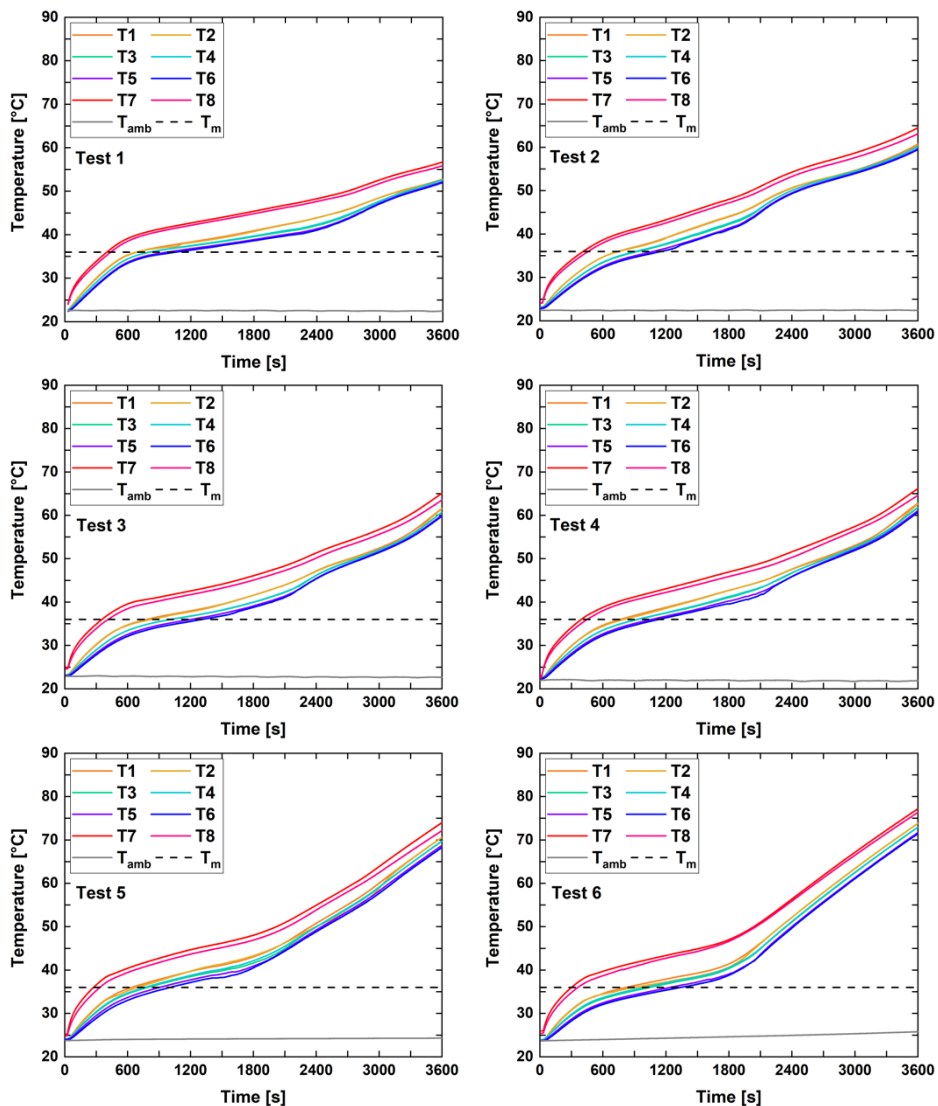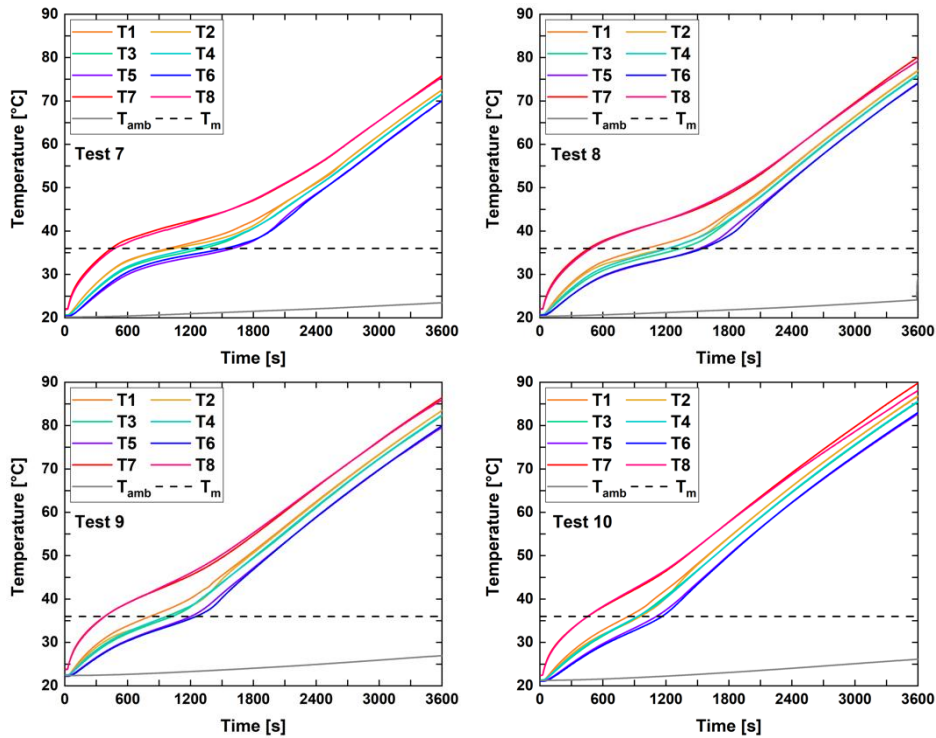
Figure 10. Phase change in case finned heat sink device

Figure 11. Free space after solidification

3.3. Phase change storage

The phase change storage ability is the most important thermal propriety of a PCM in a heat sink recipient. It can represent capability of the energy storage of a PCM. If there is a degradation of the salt proprieties, a reduction of the thermal performance and the phase change term is verified. To estimate the latent energy that can be absorbed by the salt, the energy analysis should be complete. In the Case 7 tests, the total energy (E_T) delivered was calculated neglecting the heat loads to the environment, using the following equation

$$E_T = \int_{t_1}^{t_2} Q_{el} \, dt = 270 kJ \tag{1}$$

where Q_{el} is the power supplied to the heater, t_2 and t_1 are the final and the initial time, respectively. The total energy is composed by the sensible and latent heats and is expressed as follows

$$E_T = \underbrace{\int_{T_i}^{T_m} mC_p\Delta T}_{Sensible\ heat-solid} + \underbrace{m\gamma_{sl}}_{Latent\ heat} + \underbrace{\int_{T_m}^{T_f} mC_p\Delta T}_{sensible-liquid} \tag{2}$$

where m is the mass flow in kg/s, T_i and T_f the PCM fin wall interface temperature in the beginning and in the end of the test in °C, respectively. The first term of (2) comprises the solid PCM sensible heating, up to the melting temperature. The second term is related to the solid-liquid phase change latent heat. The last part of the equation is related to the liquid sensible heating, from the melting point to up to the final temperature. Considering the phase change onset at 600s for the ten tests, when the mean melting temperature of the PCM was 36°C, the total sensible heat is the same for every test, as presented in Table 4. Each component of latent and sensible heat of the liquid, given in (1), can be calculate for the four first tests. Tests from 5 to 9 showed a

stable heat storage like test 4, and finally, for test 10 and 11 it is shown a latent heat storage degradation. The results are shown in Table 4.

Table 4. Heat distribution for each test of case 7

TEST N°	$\int_{T_i}^{T_m} mC_p\Delta T$	$m\gamma_{sl}$	$\int_{T_m}^{T_f} mC_p\Delta T$
Test 1	20.0	225.7	24.3
Test 2	20.0	215.7	34.3
Test 3	20.0	214.3	35.7
Test 4	20.0	212.9	37.1
Test 5	20.0		
Test 6	20.0		
Test 7	20.0		
Test 8	20.0		
Test 9	20.0		
Test 10	20.0		

Therefore, according to the experimental results, the phase change storage capacity decreased by less than 6% between Tests 1 and 4. However, as the number of heat cycles increases, the phase change energy decreases, reaching a small region of latent storage, depicting a reduction of almost 90% in Test 10. As heat supplied was kept the same, a slight increase of sensible heat storage is observed as the tests are performed. The fin surface temperature, T_f, increased around 13%, from 53 up to 62°C.

4. Conclusions

Two heat sink devices are experimentally studied in the laboratory to improve the knowledge of the hydrated salt sodium phosphate dibasic dodecahydrate ($Na_2HPO_4\cdot12H_2O$) thermal performance and its application conditions as PCM material. The present study provides the following main contributions:

- Inserting a metallic sponge inside the PCM material improved its thermo-physical properties and reduced the maximum surface temperature by approximately 50%.
- Fulfilling the hydrated salt at the liquid phase decreased the air content within the PCM and improved the contact area.
- Repeated tests in a row showed that four procedures decreased the latent heat storage capacity by approximately 6%. Then, its properties rapidly degraded, reducing the latent heat storage in the tenth test by 50%.
- The final temperature observed in the experimental procedures increased almost 5°C from each test to another, caused by the thermophysical properties degradation. Also, the contacting surface between the salt and heat sink decreased by 15%.

The present study showed that hydrated salt sodium phosphate dibasic dodeca-hydrate is a promising PCM material for thermal storage devices.

Acknowledgements

References

[1]   K. V. Paiva, M. B. H. Mantelli, and L. K. Slongo, "Experimental testing of mini heat pipes under microgravity conditions aboard a suborbital rocket," *Aerospace Science and Technology*, vol. 45, pp. 367–375, 2015, doi: 10.1016/j.ast.2015.06.004.

[2]   A. Gutierrez *et al.*, "Characterization of wastes based on inorganic double salt hydrates as potential thermal energy storage materials," *Solar Energy Materials and Solar Cells*, vol. 170, no. October 2016, pp. 149–159, 2017, doi: 10.1016/j.solmat.2017.05.036.

[3]   K. Vieira De Paiva, M. B. H. Mantelli, Leonardo Kessler Slongo, S. J. Burg, Raul Gohr Jr., and Victor Bissoli Nicolau, "Experimental Tests of Mini Heat Pipe, Pulsating Heat Pipe and Heat Spreader under Microgravity Conditions Aboard Suborbital Rockets," *15th International Heat Pipe Conference (15th IHPC)*, vol. 1, no. January, 2010, doi: 10.1017/CBO9781107415324.004.

[4]   A. Sharma, V. V. Tyagi, C. R. Chen, and D. Buddhi, "Review on thermal energy storage with phase change materials and applications," *Renewable and Sustainable Energy Reviews*, vol. 13, no. 2, pp. 318–345, 2009, doi: 10.1016/j.rser.2007.10.005.

[5]   M. M. Farid, A. M. Khudhair, S. A. K. Razack, and S. Al-Hallaj, "A review on phase change energy storage: Materials and applications," *Energy Conversion and Management*, vol. 45, no. 9–10, pp. 1597–1615, 2004, doi: 10.1016/j.enconman.2003.09.015.

[6]   K. Yu, Y. Liu, and Y. Yang, "Review on form-stable inorganic hydrated salt phase change materials: Preparation, characterization and effect on the thermophysical properties," *Applied Energy*, vol. 292, no. March, 2021, doi: 10.1016/j.apenergy.2021.116845.

[7]   P. Tan, P. Lindberg, K. Eichler, P. Löveryd, P. Johansson, and A. S. Kalagasidis, "Effect of phase separation and supercooling on the storage capacity in a commercial latent heat thermal energy storage: Experimental cycling of a salt hydrate PCM," *Journal of Energy Storage*, vol. 29, no. November 2019, 2020, doi: 10.1016/j.est.2020.101266.

[8]   T. X. Li, D. L. Wu, F. He, and R. Z. Wang, "Experimental investigation on copper foam/hydrated salt composite phase change material for thermal energy storage," *International Journal of Heat and Mass Transfer*, vol. 115, pp. 148–157, 2017, doi: 10.1016/j.ijheatmasstransfer.2017.07.056.

[9]   N. Kumar, J. Hirschey, T. J. LaClair, K. R. Gluesenkamp, and S. Graham, "Review of stability and thermal conductivity enhancements for salt hydrates," no. April, pp. 1–11, 2019.

[10]   V. Ahmadpour, N. Ahmadi, S. Rezazadeh, and M. Sadeghiazad, "Numerical analysis of thermal performance in a finned cylinder for latent heat thermal system (LHTS) applications," *International Journal of Heat and Technology*, vol. 31, no. 1, pp. 155–162, 2013.

[11]   L. Weiss, S. Chukwu, and E. Ogbonnaya, "Ht2012-58 Storage Device Utilizing Phase Change Materials," pp. 1–7, 2012.

[12]   S. Z. Shuja, B. S. Yilbas, and M. M. Shaukat, "Melting enhancement of a phase change material with presence of a metallic mesh," *Applied Thermal Engineering*, vol. 79, pp. 163–173, 2015, doi: 10.1016/j.applthermaleng.2015.01.033.

[13]   R. Prakash, B. Meenakshipriya, R. Kumaravelan, and S. Vijayan, "Preparation and study on thermophysical properties of inorganic salt hydrate as energy storage materials," *Materials Today: Proceedings*, vol. 42, pp. 450–456, 2020, doi: 10.1016/j.matpr.2020.10.171.

[14]   Q. Xiao, M. Zhang, J. Fan, L. Li, T. Xu, and W. Yuan, "Thermal conductivity enhancement of hydrated salt phase change materials employing copper foam as the supporting material," *Solar Energy Materials and Solar Cells*, vol. 199, no. April, pp. 91–98, 2019, doi: 10.1016/j.solmat.2019.04.020.

[15]   Y. Wang, K. Yu, and X. Ling, "Experimental study on thermal performance of a mobilized thermal energy storage system: A case study of hydrated salt latent heat storage," *Energy and Buildings*, vol. 210, p. 109744, 2020, doi: 10.1016/j.enbuild.2019.109744.

[16]   C. Nie, S. Deng, and J. Liu, "Numerical investigation of PCM in a thermal energy storage unit with fins: Consecutive charging and discharging," *Journal of Energy Storage*, vol. 29, no. January, p. 101319, 2020, doi: 10.1016/j.est.2020.101319.

[17]   S. Işık and C. Yıldız, "Improving thermal energy storage efficiency of solar collector tanks by placing phase change materials in novel finned-type cells," *Thermal Science and Engineering Progress*, vol. 19, no. June, 2020, doi: 10.1016/j.tsep.2020.100618.

[18]   N. Stathopoulos, G. Belessiotis, P. Oikonomou, and E. Papanicolaou, "Experimental investigation of thermal degradation of phase change materials for medium-temperature thermal energy storage and tightness during cycling inside metal spheres," *Journal of Energy Storage*, vol. 31, Oct. 2020, doi: 10.1016/j.est.2020.101618.